AIAA 80-0300R

A Cooled Laminated Radial Turbine Technology Demonstration

Roy W. Vershure Jr.,* Gerold D. Large,† and Leonard J. Meyer‡
The Garrett Turbine Engine Company, A Division of The Garrett Corporation, Phoenix, Ariz.
and
Jan M. Lane§
U.S. Army Research and Technology Laboratories (AVRADCOM), Ft. Eustis, Va.

A low-cost, high-temperature radial turbine has been developed demonstrating the technology required to manufacture a small, cooled turbine using photoetched laminates bonded together to form a complete wheel. An advanced long-life, high-performance turbine design is described which uses an iterative optimization procedure to provide a balanced mechanical and aerodynamic design. The design efficiency was 87.2%, with a predicted life of 8500 h in stress rupture and a low-cycle-fatigue life of 7600 cycles. The calculated bulk heat-transfer effectiveness was 0.54 with operation at 2300°F. Several wheels were manufactured from Astroloy, and the mechanical integrity was demonstrated in a series of proof tests conducted in a whirlpit test facility.

Introduction

THE radial inflow turbine has proven to be a very attractive component for small Army gas turbine engines. The concept of radial entry and axial discharge, both on paper and in actual engine operation, has clearly demonstrated a capability to utilize hot-gas energy beyond the levels that small axial turbines can accommodate and in a more efficient manner. For engines with airflows of approximately 5 lb/s or less, the radial turbine permits somewhat higher-cycle pressure ratios with higher turbine and cycle efficiencies at essentially equivalent turbine inlet temperatures. This permits reduced fuel consumption while also reducing the number of parts, engine length, and cost. Though the use of radial turbines has been limited (basically because of geometric/flow constraints on engine size), the primary limitation has been fabricability and the constraint to operate at lower turbine inlet temperatures consistent with uncooled designs machined from forgings or integral castings.

The need for increased cycle performance and further reduced fuel consumption for Army gas turbines dictates the requirement for higher turbine inlet temperatures—2300-2500°F appears to be an attractive goal. In the absence of advanced materials such as ceramics, the extension of cooling technology from axial turbines has been attempted; however, the design approaches integrated with fabrication technology have been fraught with difficulty. It has been shown, nonetheless, that a single radial turbine operating at elevated temperatures can generate sufficient work to produce attractive cycle pressure ratios and significant reductions in fuel consumption.

Additionally, it has been concluded that, for high-temperature operation including cooled blading, the single-most critical parameter limiting radial turbine performance is stress distribution. Rotor stresses limit the achievable tip speeds to nonoptimum levels due to excessive bore stresses, particularly in the presence of front-drive power turbine shafting, causing sizable wheel-bore diameters. Rotor stresses also force the designer to utilize radial blade sections to prevent additional bending loads superimposed on already high centrifugal blade stresses. This creates nonoptimum incidence at the rotor inlet.

Early in 1967 several other potential solutions to the cooled radial turbine fabrication problem surfaced. Both in-house and government-funded efforts at several locations indicated new fabrication technologies existed that could be scaled up to production processes for fabricating these rotors. While casting technology had also advanced, it was clear that in order to provide realistic bore diameters under properly imposed fatigue life and burst requirements, wrought properties in the bore are necessary to achieve maximum tip speeds. An Army program was initiated to evaluate improved fabrication technology for long-life, high-temperature radial turbines, and two contracts were awarded. It is the desire of the Applied Technology Laboratory to fully evaluate and document this fabrication potential to provide the necessary tools for incorporation of radial turbines in advanced fuel-conservative engines. This paper describes the design and development testing at Garrett that led to the manufacture and testing of the first cooled, laminated, integral radial turbine (Fig. 1).

Design

The cooled radial turbine was designed to meet several major engine requirements, namely: adaptable to front-drive power-turbine applications and a radial turbine matched to a high-work, high-pressure-ratio centrifugal compressor.

Figure 2 is a conceptual layout of a small turboshaft engine that utilizes a single-stage centrifugal compressor driven by a cooled radial turbine. A reverse-flow annular burner is employed to take advantage of the radial turbine flowpath. This effectively provides the Army with a simple and compact engine with a minimum number of turbomachinery components and takes full advantage of a cooled radial turbine configuration in a small turboshaft engine.

Design Requirements

In the smaller flow-class engines, analytical studies and experimental data have shown the performance superiority of radial turbines compared to their axial counterpart. The radial turbine should be ideally suited for the gas generator turbine for these applications. Unfortunately, the inability to internally cool the radial rotor has been a significant deterrent

Presented as Paper 80-0300 at the AIAA 18th Aerospace Sciences Meeting, Pasadena, Calif., Jan. 14-16, 1980; submitted April 24, 1980; revision received March 2, 1981.

*Development Specialist, Advanced Technology Propulsion Engineering. Member AIAA.
†Senior Supervisor, Aero/Thermo Component Design. Member AIAA.
‡Supervisor, Mechanical Component Design.
§Aerospace Engineer, Applied Technology Laboratory.

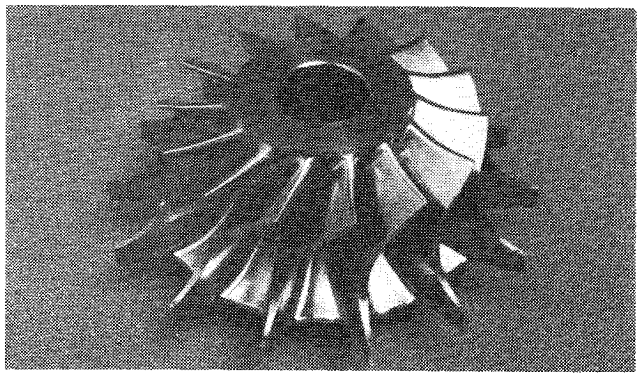

Fig. 1 Garrett cooled laminated radial turbine.

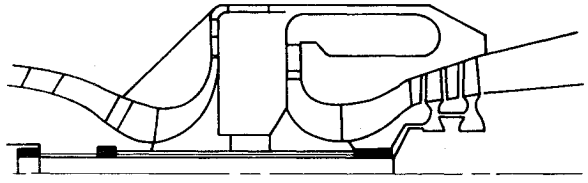

Fig. 2 Cross section of concept engine.

to the use of radial turbines and the amount of aerodynamic research devoted to the radial turbine. However, the development of laminated construction techniques will not only eliminate this constraint but will increase the performance potential of future small turbofan and turboshaft engines.

The conceptual engine configuration that was established combines the characteristics of a small, advanced centrifugal compressor of about 3 lb/s mass flow with the cooled radial turbine to produce a turboshaft engine with the turbine design requirements listed in Table 1.

Aerodynamic Design

Preliminary Design Analysis

In recent years, both the attainable radial turbine efficiency and the degree of accuracy of the prediction techniques have rapidly increased. At Garrett, this was due to the number of new designs recently developed for a wide range of applications which have allowed new correlations to be developed from rig test programs. These programs have, in conjunction with the extensive analytical and experimental investigations conducted by NASA,[1,2] resulted in the evolution of an accurate method for evaluating the performance potential of radial turbines. The most significant correlations derived from the experimental data are: 1) that peak efficiency will occur at an inlet work coefficient that is consistent with the centrifugal compressor slip factor developed by Stanitz[3] and 2) that the reduction in peak efficiency at higher or lower work coefficients can be accurately accounted for by a rotor inlet incidence loss that is calculated from the difference in kinetic energy between the actual and optimum inlet work coefficients. The first result can then be utilized to obtain a relationship between turbine stage work and the required tip speed for peak efficiency. Figure 3 shows this relationship for a range of blade number based on zero rotor exit swirl. At the specific work required by the laminated radial turbine, the inducer tip speed required to achieve peak efficiency is between 2175 and 2310 ft/s for a blade number between 10 and 20. Based on previous radial turbine designs, the allowable tip speed is expected to be between 1800 and 2000 ft/s with current material properties and the large bore diameter required for a front-drive turbine. Therefore, Fig. 3 shows that the laminated radial turbine will be tip-speed limited, resulting in rotor-inducer incidence losses.

Table 1 Turbine design requirements

Rotor inlet temperature, °F	2,300
Corrected specific work, $\Delta H/\theta$, Btu/lbm	32.0
Minimum cooled efficiency, η_{T-TC}, %	86.0
Rotor inlet corrected flow, $W\sqrt{\theta}/\delta$, lb/s	0.633
Total-to-total pressure ratio, $(P/P)_{T-T}$	3.3
Rotational speed, N, rpm	73,380
Minimum design life, h	5,000
Minimum operational low-cycle-fatigue (LCF) life, cycles	6,000

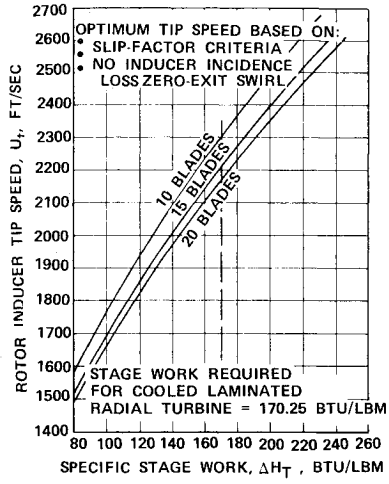

Fig. 3 Optimum tip speed as a function of stage work and blade number.

To reduce the rotor inlet incidence losses associated with high-work radial turbine designs, two approaches are feasible. The first is to adjust the inducer-to-exducer work split to allow optimum rotor inlet conditions to be reestablished; that is, negative rotor exit swirl. In principal, rotor inducer incidence would be eliminated; however, in practice, this solution transfers the losses to the rotor exducer and the downstream interturbine duct due to the increase in rotor exit Mach number and swirl. A favorable tradeoff between rotor inducer incidence loss and rotor exit and interturbine duct loss is possible by adjusting the inducer-to exducer work split for tip-speed-limited turbine designs. This type of analysis, however, requires definition of the downstream interturbine duct and power turbine and was beyond the scope of this program. The second approach, and the one selected for the cooled, laminated radial turbine, is to optimize the vector diagram based on minimizing the total losses between rotor inlet incidence and exit swirl losses. This assumes the rotor exit tangential kinetic energy is lost. This type of analysis is considered desirable for the present design, since this method does not arbitrarily favor the turbine efficiency at the expense of unduly increasing the interturbine duct loss, and in addition, maintains high-rotor reaction.

This optimization procedure was applied to the cycle requirement of the cooled radial turbine for a range of rotor tip speeds and blade number during the preliminary design phase of the program. For this analysis, the performance with internal cooling flow was calculated by assuming all the cooling flow discharges at the rotor exit trailing edge, and the uncooled turbine efficiency was adjusted by a pumping penalty based on the rotor exit mean wheel speed. The result of this analysis is presented in Fig. 4. Based on rotor life requirements, mechanical analysis of these solutions indicated that the maximum allowable rotor tip speed was 1880 ft/s. At this condition, 14 blades are required to achieve the efficiency goal of 86.0%.

Turbine Efficiency Prediction

Historically, radial turbine performance has been based on a specific speed correlation[2,4-6] or on a detailed evaluation

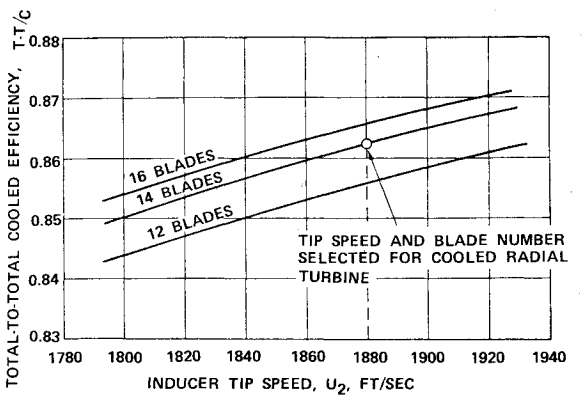

Fig. 4 Preliminary design optimization study for cooled laminated radial turbine.

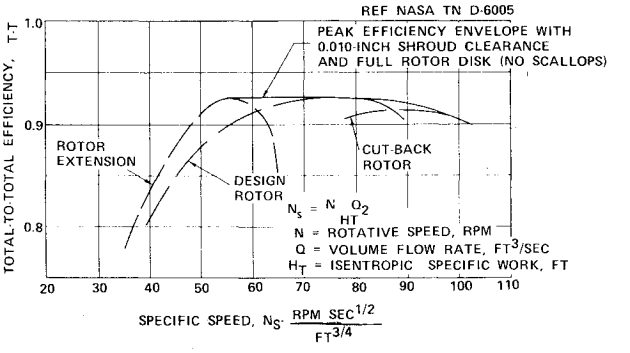

Fig. 5 Composite turbine performance.

based on loss coefficients derived from previous test results.[1,7-9] Although significant progress has been made in terms of identifying the conditions for peak efficiency and modeling the effects of rotor inducer incidence due to the nonoptimum inlet conditions, all methods currently utilized suffer from the basic inability to accurately predict the profile and secondary flow losses in radial turbines. The problem is a result of both the complex three-dimensional flow and the unusually high number of design parameters that must be evaluated in order to arrive at meaningful correlations. Rig testing is also complex and expensive, which tends to limit the availability and dissemination of radial turbine data. However, current developments in flow visualizations and three-dimensional viscous flow calculation techniques should significantly increase the capabilities for correlating radial turbine internal losses.

The basic model for a comprehensive radial turbine design analysis and performance prediction technique has been developed by Glassman.[9] This analysis not only accounts for the basic stator and rotor geometry, which is required to evaluate the profile and the secondary flow losses, but equally important, it performs a two-dimensional flow analysis at the rotor exducer that is required to evaluate rotor exducer blockage, deviations, and rotor loading. When more general correlations become available for stator and rotor losses, Glassman's methods can be expanded to arrive at a sophisticated method for radial turbine performance predictions. The current approach utilized at Garrett is a combination of the two basic methods; that is, a specific speed correlation is used to obtain the base efficiency at zero clearance and reference Reynolds number, and then in-house correlations are used to evaluate the additional losses that will be present. One of the most comprehensive experimental programs conducted to evaluate the effects of specific speed on radial turbine performance was due to Kofskey and Nusbaum at NASA.[2] This program examined the maximum attainable efficiency as a function of five stator geometries (varying throat areas), and three rotor configurations (baseline, extended exducer, and cutback exducer). The results showed the maximum total-to-total efficiency envelope (based on the combination of the three rotor configurations) could be defined, which would result in peak efficiencies of 92.5% over a range of specific speeds from 55 to 85, as shown in Fig. 5.

Although these results are for a relatively low-stage-pressure-ratio design, correlation of Garrett's higher-pressure-ratio designs indicate that these same peak efficiency levels could still be achieved. The specific speed of the cooled, laminated radial turbine is 69.0, and at zero clearance the peak efficiency is 94.8. Additional losses that must be accounted for to arrive at the final predicted cooled total efficiency are listed and summarized in Table 2.

The effects of rotor cooling flow on turbine performance are usually accounted for by assuming that all internal and

Table 2 Cooled-turbine efficiency prediction

Aerodynamic efficiency	η_{T-T}	$\Delta\eta_{T-T}$
Base efficiency from specific speed correlation	0.948	
Reynolds number effect at $R_E = 3.5 \times 10^5$	0.949	+0.001
Rotor inlet incidence effects	0.921	−0.028
Rotor shroud clearance effects at 0.012-in. clearance	0.898	−0.023
Rotor backface clearance effects at 0.030-in. clearance	0.889	−0.009
Blade number effects with 14 blades	0.884	−0.005
Rotor backface disk friction effects	0.881	−0.003
Rotor exit blockage effects	0.872	−0.009
Final predicted aerodynamic efficiency	0.872	
Cooled efficiency	$\eta_{T-T\text{cooled}}$	$\Delta\eta_{T-T}$
Rotor backface cooling for 0.60% cooling flow based on test results	0.872	0.0
Rotor internal cooling flow at 4.94% cooling flow, based on axial turbine tip discharge test results	0.872	0.0
Final predicted cooled efficiency	0.872	
Design requirement	0.860	

disk cooling flows do not work in passing through the turbine and that pumping work is required to accelerate the cooling flows to wheel speed. For the preliminary design analysis, the rotor internal cooling flow penalty was based on pumping the flow to rotor exit mean wheel speed, since a trailing-edge discharge scheme was anticipated. However, during the detail design phase, the cooling flow scheme was modified. The final scheme results in all cooling flow discharge to the rotor shroud and backface clearance regions. Test data evaluating the effects of tip discharge is currently not available for radial turbines, but has been investigated for axial turbines. The results show the cooled turbine efficiency either remains constant or rises slightly up to 3.0% internal cooling. This characteristic is attributed to a reduction in tip-clearance losses, which offsets the required internal cooling flow pumping requirements. The same beneficial effects are expected to occur in the radial turbine, especially in the exducer region where similarities between the axial and radial turbine blading are the greatest.

The effects of rotor backface cooling flow have been investigated at Garrett for a range of cooling flow up to 6%. This cooling flow is required to prevent high-temperature mainstream flow from recirculating in this region. Test results showed that the work done by the cooling flow (after entering the turbine flowpath at the scallop region), due to acceleration through the rotor, offsets the required pumping work done on the rotor backface.

This conclusion is based on two methods of calculating the cooled turbine efficiency. The first method derives the turbine work based on the thermodynamic mixing of both cooling and mainstream flows. The second method is based on calculating the turbine work from the Euler work equation by integrating the rotor exit radial work distribution with cooling flow and calculating the rotor inlet tangential velocity from a constant stator loss coefficient obtained without rotor cooling.

The internal cooling flow geometry has also resulted in a significant increase in blade thickness compared to a conventional uncooled radial rotor. Test results on the effects of rotor trailing-edge blockage on overall performance do not appear to be available in the open literature, although the problem was recognized by Rogers.[10]

The rotor-exit hub blockage of Garrett turbines used in the specific speed correlation of NASA data is on the order of 30%. However, the required blade thickness of the cooled radial turbine results in an exit hub blockage of approximately 50%. Although rotor-exit survey data indicate the radial turbine is less sensitive to blockage compared to the axial turbine, an order-of-magnitude effect of the increased blockage was evaluated based on a mixing loss calculation that accounted for the blade thickness. The loss calculation was performed for both the laminated radial and for a previously tested radial turbine with approximately 30% hub blockage, which matches the NASA peak-efficiency curve.

The mixing loss calculations were based on the incompressible dump-loss correlations developed by Benedict.[11] The difference in mass average relative total pressure between the subject and reference turbine was 1.16% ($\Delta P/P$), which translates to an overall efficiency decrease of 0.90 point, as shown in Table 2. The incompressible results were compared with a two-dimensional compressible mixing loss based on the Stewart[12] method, and the same magnitude of total pressure loss was obtained.

Detailed Rotor Aerodynamic Design

The rotor inlet and exit flowpath dimensions were established from the optimized one-dimensional vector diagram. The detail rotor design is initiated with preliminary estimates of hub and shroud contours, blade thickness, and angle distributions. These quantities are input to a radial turbine geometry program along specified station lines (quasiorthogonals for the internal flow solution). The resultant data matrix is curve-fitted to define the total blade geometry. The computer program is a modification of a current centrifugal impeller geometry program, which allows an arbitrary blade to be defined. Once the final blade geometry is established, the required tooling section coordinates are calculated for manufacturing drawings.

In order to perform the internal flow analysis, the level and distribution of losses in the rotor must be specified in addition to the rotor blade geometry and thermodynamic conditions. The magnitude of the total stage loss is determined from the efficiency analysis described earlier. The stator loss is estimated from previous turbine rig tests with the remaining loss assigned to the rotor.

The distribution of rotor losses, both in the flow-through and radial directions, is more difficult to establish. Because of the lack of detailed knowledge of the internal rotor flowfield, the losses in the flow-through direction are assumed linear. For the radial direction, a loss distribution based on recent test data from a radial turbine of similar size and pressure ratio was utilized.

The computer program for the rotor internal flow analysis solves the radial-equilibrium equation by satisfying the continuity, momentum, and energy equations in the meridional plane in a manner similar to Refs. 13 and 14. Blade surface velocities are then computed from the local rate-of-change in moment of momentum, the condition of zero-absolute vorticity, and linear velocities between suction and pressure surfaces. Stanitz[15] has shown that this method produces satisfactory results compared with relaxation solutions of the potential-flow equation. A number of iterations between the geometry program and internal flow analysis program are required to achieve satisfactory blade loading for each thickness distribution examined.

The criteria for satisfactory blade loadings are monotonically increasing velocities and minimum blade surface diffusions. For highly loaded rotors (which normally implies increased loading and incidence in the rotor inducer region), this criterion is not satisfied. In addition, inlet flow deviations based on Stanitz's criteria are not expected to apply; therefore, the loadings in the inducer region become ill-defined. Under these conditions, it is doubtful that more rigorous stream-function methods for evaluating the blade surface velocities are warranted.

Mechanical Design

Cooling Configuration Synthesis

The requirements demanded of a radial turbine cooling system design depend upon three variables: the operating environment and stress level, the required life and mission, and the material capabilities. For this application with a mission life requirement of 5000 h, with 1000 h at maximum rated power, and with the selection of Astroloy material for the laminates, the operating stress levels indicate a need for an efficient and sophisticated cooling system. A design goal was set for a blade-metal temperature reduction of 500°F below the uncooled blade prediction for this configuration. Using the laminate process permits the designer a maximum degree of flexibility in choosing an internal cooling configuration which optimizes the internal heat transfer with precise flow control.

Several cooling-scheme configurations were investigated during the design, and each was judged for its efficient distribution and allocation of cooling flow, maintenance of structural integrity, minimization of thermal gradients, and overall simplicity. Configuration 1 of Fig. 6 is a two-passage, single-pass, meridional flow scheme. While it offers simplicity and ease of flow control, its shortcoming is almost complete reliance on trailing-edge discharge. With the high turning angle of the blade exducer, trailing-edge discharge requires excessive blade thickness to create sufficient flow area at the laminate interface locations, and the associated aerodynamic blockage becomes an insurmountable problem. Configuration 2 is a modification that utilizes radial flow and tip discharge in the exducer to overcome the trailing-edge thickness problems. Further evaluation of this design showed promise, but the very high level of coolant-side heat transfer required in the inducer leading edge was unobtainable without further changes. Configuration 3 is a design modification that incorporates impingement cooling in the inducer leading edge to achieve satisfactory metal temperature levels. Also, better flow control and heat-transfer augmentation are achieved in this design by utilizing internal baffling and pin fins. The selected design, shown in Fig. 7, includes a serpentine passage in the exducer for greater thermal efficiency and reduction of cooling air usage. This design was subjected to further optimization and detailed analysis.

Thermal Design Analysis

The heat-transfer and pressure-drop characteristics of laminated-blade cooling passages are higher than for smooth-walled passages because of the inherent roughness which varies according to laminate orientation with respect to flow direction. Experimental work on roughness effects in threaded passages has been utilized to develop correlations for friction factor and heat-transfer rate in these rough passages.[16-19] Passage-roughness to hydraulic-diameter ratio correlations indicate increases in actual friction factors of 480% and increases of wall heat-transfer rate of 140%.

Early in the design process it became clear that an in-depth detail analysis was required to achieve the desired flow

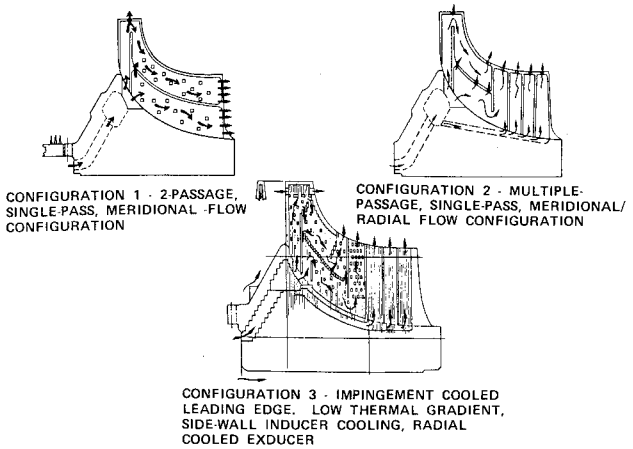

Fig. 6 Candidate cooling scheme configurations.

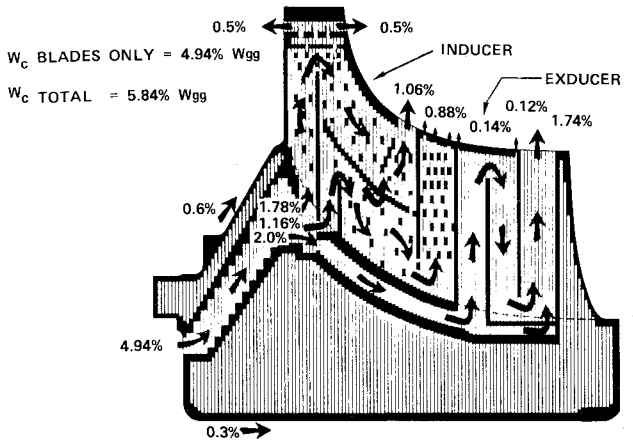

Fig. 7 Cooling geometry.

distributions within a multiplicity of series and parallel-connected passages. Compressible flow network analysis has been utilized to account for heat-transfer effects, fluid friction, rotational forces, fluid transport properties, and geometry effects. Geometric features presented in this design include rectangular pin fin arrays of varying densities, metering and cross-passage bleed holes, passage height variations, and flow guides. In conjunction with computer solutions for fluid temperatures and pressures within the cooling circuit, a heat conduction solution yields airfoil wall internal and external surface temperatures. External thermal boundary conditions were calculated at the maximum power condition from aerodynamic data and airfoil geometry using standard methods and a flat inlet temperature profile.

As presented in Fig. 7, the airfoil inducer cooling design includes an upper and lower circuit handling together 2.94% of core flow. Pin fins are used extensively for heat-transfer augmentation, and the leading edge has a preorificed impingement feature with impingement air discharge at both shroud lines. This leading-edge design provides for adequate flow discharge if a shroud rub occurs, negligible performance penalty from the flow discharge, and erosion or foreign object damage tolerance. Both upper and lower circuits are oriented to have coolant temperature increasing as external temperature decreases with lower blade radius, thereby reducing wall thermal gradients. Blade-tip discharge is employed with attendant performance benefits due to effective tip-clearance reduction.

The cooled blade exducer uses 2.0% of core flow supplied in equal portions to each of 14 blades by separate passages in the wheel hub. A serpentine three-pass design was selected over the three-passage design because of its greater thermal efficiency; it required 60% less cooling flow to produce

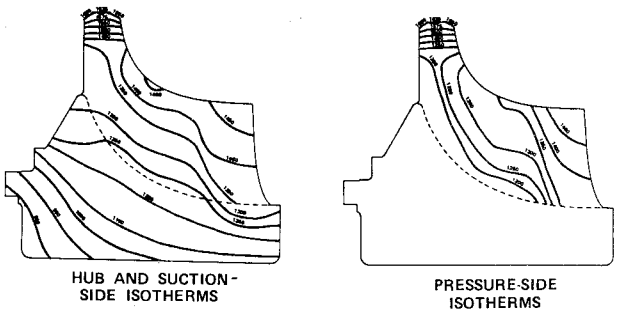

Fig. 8 Steady-state temperature predictions.

similar peak metal temperatures and reduced-wall thermal gradients. The greater thermal efficiency is derived primarily from higher average flow velocities, second-pass flow direction oriented toward decreasing external-gas temperatures, and third-pass augmentation flow balancing wall temperatures evenly between all three passes.

The cooled radial wheel temperature predictions for steady-state conditions at maximum power and turbine inlet temperature are presented in Fig. 8. These predictions were used for stress and life analysis of the turbine. The bulk average metal temperature for the cooled laminated rotor was 1325°F, indicating an effective cooling design has been attained.

A very high bulk-heat-transfer effectiveness $\eta_b = 0.54$ was calculated based on the relative turbine inlet temperature of 2000°F and the rotor cooling air inlet temperature of 750°F as defined below:

$$\eta_b = \frac{T_{\text{relative in}} - T_{\text{metal bulk}}}{T_{\text{relative in}} - T_{\text{cooling}}} = \frac{2000 - 1325}{2000 - 750} = 0.54$$

Design Iteration

The final radial turbine design is the result of the close-coupled optimization of many competing design parameters encompassing mechanical integrity, life, aerodynamic performance, and thermal behavior considerations. An iterative process is required in the design to ensure that none of the considerations are jeopardized in deference to another. This process centers around the rotor airfoil geometry, and is initiated within established flowpath constraints by approximations of the blade thickness distribution, which lead to aerodynamic blockage and efficiency estimates, blade-cooling design and temperature predictions, stress-rupture life predictions, airfoil natural frequencies of vibration, burst margin, and finally, low-cycle-fatigue life predictions. During the iterations, experience gained from other Garrett radial-turbine designs was utilized to narrow the constraints. Blade trailing-edge root fillet design and saddle region fillet design are two areas that received substantial attention as a result of service experience with radial turbines.

As blade geometry definition was refined to successive levels during the design process, the disk geometry was adjusted to maintain reasonable levels of localized stress and to achieve adequate burst margin. The influence of physical constraints such as curvic coupling extensions and balance material were included early in the design process along with the wheel-bore diameter restrictions controlled by the Army requirement for a front-drive turboshaft engine configuration. When analysis and experience factors dictated that a balanced design has been achieved by all appropriate criteria, the iterative phase was concluded, and more detailed analysis was undertaken.

Analysis Results

During the iterative design process, analytical evaluation was accomplished using two-dimensional approaches. For detailed mechanical design analysis, the two-dimensional finite-element treatment of the rotor with blades described as

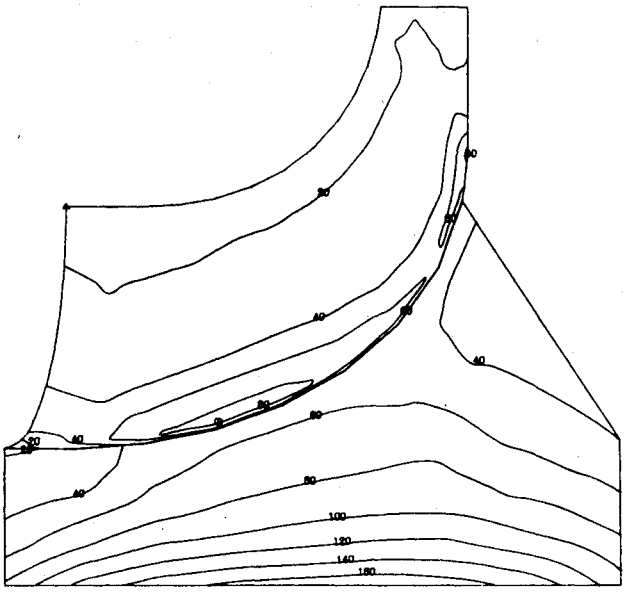

Fig. 9 3-D equivalent stresses (ksi) for combined effects of rotation (73,380 rpm) and temperatures on blade suction surface and corresponding disk.

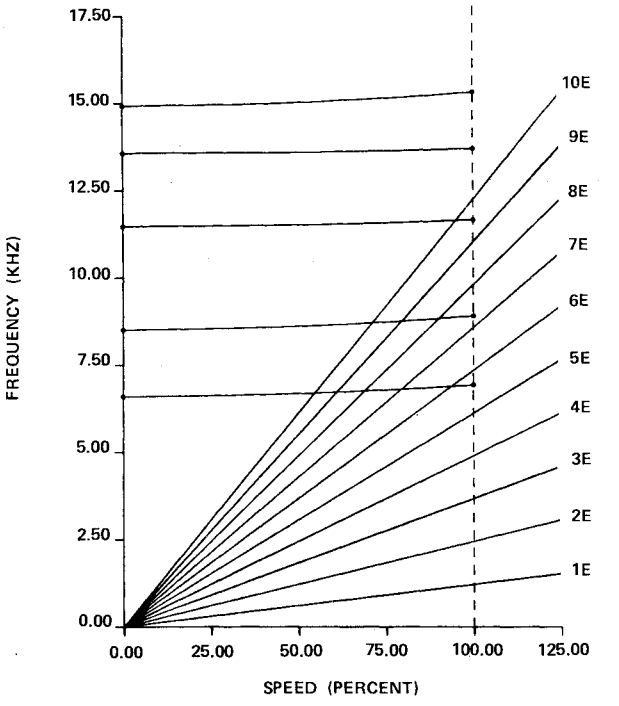

Fig. 10 Campbell diagram for first five natural frequencies at steady-state operating temperatures.

plane-stress elements was retained as the optimum method for evaluation of the hub portion of the wheel. For the blade and blade-to-hub interface region, a three-dimensional, finite-element elastic stress analysis was utilized to obtain better resolution of stress concentrations arising from the complex geometry and the temperature gradients.

Rotor-hub stress analysis led to optimization of the coolant supply passage position and size for burst margin considerations, and to the use of an elliptical inlet passage hole to reduce stress concentration effects. Stresses were obtained from the two-dimensional analysis for a condition of maximum operating speed at room temperature. The average tangential stress achieved is 82.8 ksi. A burst margin of 31% was calculated using a material utilization factor of 0.85, and a minimum ultimate tensile strength of 167 ksi at a rotor hub average temperature of 1200°F. In the presence of maximum-power condition steady-state temperatures, the peak bore equivalent stress increased to 175 ksi from 140 ksi for rotation only.

The three-dimensional analysis predictions for equivalent stress at the maximum-power condition on the external suction side surface is presented in Fig. 9. Peak stresses slightly above 80 ksi occur in the blade exducer fillet region on both suction- and pressure-side surfaces.

Stress-rupture life of the turbine blade has been predicted using conservative factors on both local metal temperatures and rotation stress levels. Minimum stress-rupture properties of forged Astroloy were used in the calculation since materials testing conducted to date has indicated an equivalency with laminate in-plane properties. A minimum expected stress-rupture life of 8500 h was calculated with all of the significant life consumed at the 100% rated power conditions. The minimum low-cycle-fatigue life prediction of 7600 cycles at the bore peak stress location was made using steady-state peak stresses in the absence of transient solutions and using low-cycle-fatigue data from axial strain controlled test specimens of forged Astroloy at the appropriate local temperatures.

A three-dimensional, finite-element blade vibration analysis has been conducted with temperature and centrifugal stiffening effects included. The fundamental frequency is between the fifth and sixth engine orders at 100% operating speed, as shown in Fig. 10. Garrett experience on other radial wheels indicates that the likelihood of vibration problems surfacing in this frequency range in minimal.

A possible mode of failure attracting more attention in laminate structures than in traditional castings and forgings is flaw-initiated crack propagation to critical size and growth rate. In the rotor hub flaws at bond joints would be propagated most easily along the bond, but axial stresses that would control the growth rate in the bond joint are generally quite low. Transverse to the bond joints, the potential cracks would be propagated by radial and tangential stresses, but Astroloy material characteristics in the laminates include excellent subcritical crack-growth resistance and fracture toughness. In the rotor blades, the propagation of flaws along bond joints from the combined presence of thermal stress and vibratory stress is of primary concern, but analytical predictions of vibratory stress amplitude are difficult to accomplish and must, therefore, await strain-gage testing of the rotor in an actual engine environment.

Laminate Manufacturing Process

The Garrett laminate manufacturing process that was originally developed and tested under Air Force sponsorship[20,21] is illustrated in Fig. 11. The illustration shows the basic process operations applied to a radial turbine starting with an 0.020-in. Astroloy sheet that is chem-milled to a precision thickness prior to photoetching the laminates. The radial wheel blank contains 141 laminates with 92 different cooling passage configurations. The passages were accurately generated using computer-aided design techniques that define each passage with straight-line elements and with an x/y digitized coordinate system at each Z section. To ensure stability, the final 1:1 size Z section tooling master is developed on a photosensitive glass plate to a tolerance of less than ± 0.001 in. and subsequently transferred to a Mylar photopositive for each laminate. Actual dimensional inspection of laminate details indicated an average variation from true position of ± 0.0003 in. After the laminates are photoetched, they are thoroughly cleaned to remove all oxides and organic contaminates that could potentially have an adverse effect on the bond joint integrity.

Next, alternate laminates are boron-coated using the Borofuse process. Borofuse is a proprietary process of diffusing boron into the base metal surface under controlled conditions to obtain the desired boride density that reduces the melting point temperature at the bond interface. The laminates are stacked, bonded, and heat-treated in a vacuum

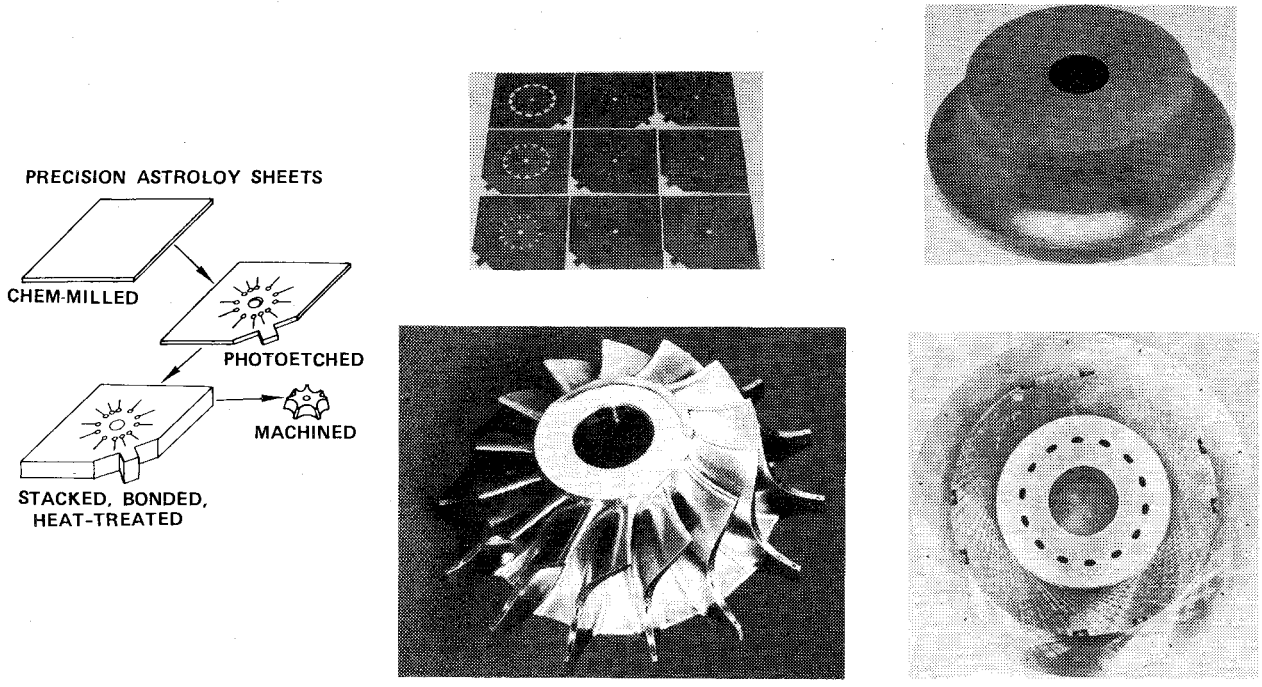

Fig. 11 Garrett laminate manufacturing process.

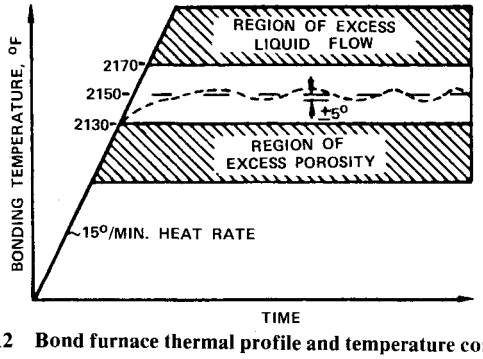

Fig. 12 Bond furnace thermal profile and temperature control.

furnace at 2150°F for 2 h, while maintaining a constant 100 psi unit loading. A typical bond furnace thermal profile is presented in Fig. 12. Acceptable diffusion bonding occurs in the 2130-2170°F bond-temperature range with a 15 deg/min heating rate. A microprocessor controller is utilized to maintain the accurate temperature control required. This effectively avoids either an overtemperature bond, which produces excess liquid flow and subsequent cooling passage blockage, or an undertemperature bond, which produces excess porosity with reduced bond joint mechanical integrity.

The basic nondestructive evaluation (NDE) on the wheel blank is an ultrasonic inspection, which is performed to check the bond joint integrity. Also, test specimens are removed from excess stock in the wheel blank to establish the mechanical properties and to examine the bond joint microstructure.

The wheel blank is premachined to expose the blade cooling air passages in order to conduct an in-process blade airflow test on the bench prior to final machining. The blade profile machining is completed using single-spindle duplicating methods. However, it is anticipated that electrochemical machining (ECM) methods will be used in production.

Mechanical Integrity Testing

The mechanical integrity tests were performed on the laminated radial wheel and consisted of an airflow test; a stresscoat test; a growth, overspeed, and burst test; and several cyclic endurance tests in a whirlpit test facility to access the low-cycle-fatigue life.

Airflow Test

An in-process airflow test of the laminated radial wheel was completed prior to final blade profile machining. A minimum flow variation blade-to-blade of ±4.2% was achieved. This compares favorably to cast-inserted blades, which have an allowable variation of ±10%. Also, zero leakage was demonstrated with the blade cavity air pressurized in a submerged water tank test. This simple in-process test procedure established the overall integrity and conformity to the design of the cooled rotor prior to final blade profile machining.

Stresscoat Test

The purpose of the stresscoat test was to evaluate regions of high-stress concentration in the rotor. This test was conducted in the whirlpit test facility at reduced speeds (50 and 55 rpm), and under carefully controlled temperature and humidity conditions. The stress patterns developed are shown in Fig. 13 and occur primarily in the blade fillets. Note that small local stress concentrations occurred on several blades in the inducer-tip region of the S/N 2 rotor. These concentrations correlated with known Zyglo and porosity indications previously established on the rotor.

Growth, Overspeed, and Burst Test

The laminated wheel was growth-tested in order to determine the response of the wheel structure to overspeed conditions and to evaluate the burst speed margin. A maximum total growth of 0.008 in. occurred in the bore under the inducer portion of the disk. The actual burst speed was 92,200 rpm, 126% of the design speed, which is slightly below design burst speed of 131%. A three-piece hub burst occurred, which is typical of a homogeneous isotropic material, and post-test mechanical properties were verified in the bore.

Cold Cycle Testing

A cold cycle test is planned in the whirlpit test facility to evaluate the mechanical fatigue strength of the radial laminated wheel. Since the proper thermal gradients in the

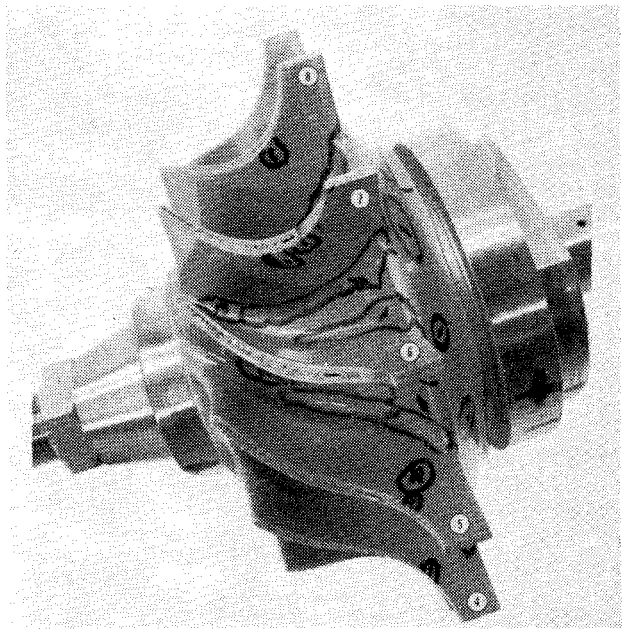

Fig. 13 Stresscoat test results, S/N 2 rotor.

wheel cannot be duplicated, except in an engine environment, only the mechanical or centrifugal loading will be generated. Overspeed cycles to about 120% of design speed will be used to compensate for the lack of thermal environment. On the basis of whirlpit testing of forged nickel-based turbine wheels at 70°F, no crack initiation or failure is expected in 6000 cycles. Inspections will be performed at intermediate cycles using Zyglo and visual inspection methods to detect any cracks that may develop.

A preliminary cycle test was conducted on the S/N 2 rotor up to 100% design speed to check for a change in the blade porosity indications and stress concentrations identified in Zyglo and stresscoat. Dimensional and Zyglo inspections at 1, 10, 35, 100, 200, 350, and 500 cycles were completed. No change occurred in the porosity indications; a slight change occurred in the bore and tip diameters (±0.0002 in.). Zyglo inspection of the bore and disk were clean and free of defects.

Summary and Conclusions

A small, high-temperature, cooled radial turbine rotor has been designed for operation at 2300°F and manufactured utilizing the Garrett laminate process. The laminate design established represents a good balance between aerodynamic and mechanical design which satisfies the major Army design requirements. That is, a design efficiency of 86% vs a predicted efficiency of 87.2%; a design life of 5000 h vs a predicted life of 8500 h in stress rupture; and a low-cycle-fatigue life of 6000 cycles vs a predicted life of 7600 cycles. Also, the maximum metal temperature at the blade tip was held at 1650°F with a bulk average temperature of 1325°F. The inherent flexibility of the laminate process has provided an optimized blade cooling design with a high bulk-metal effectiveness of 0.54.

A series of whirlpit tests was conducted to evaluate the mechanical integrity of the rotor. These tests included overspeed, growth, and burst testing up to 126% speed and a stresscoat test to evaluate stress concentrations. Further cyclic testing is planned in order to establish the low-cycle-fatigue characteristics of the rotor.

In conclusion, this program has demonstrated the feasibility of manufacturing a high-temperature, cooled radial turbine utilizing the Garrett laminate process. The application of cooled integral radial turbines in small propulsion engines should lead to more fuel-efficient engines in the future.

Acknowledgments

The authors wish to recognize the valuable contributions to the turbine design of G.W. Bowers, M.J. Egan, D.G. Finger, J.C. Mays, J.T. Sublett, and M.H. Willmore. This work was performed under U.S. Army Contract DAAJ02-77-C-0032 for the U.S. Army Research and Technology Laboratories, Fort Eustis, Va.

References

[1] Rohlik, H. E., "Analytical Determination of Radial Inflow Turbine Design Geometry for Maximum Efficiency," NASA TN D-4384, 1968.

[2] Kofskey, M.G. and Nusbaum, W.J., "Effects of Specific Speed on Experimental Performance of a Radial Inflow Turbine," NASA TN D-6005, Feb. 1972.

[3] Stanitz, J.D., "Some Theoretical Aerodynamic Investigations of Impellers in Radial and Mixed-Flow Centrifugal Compressors," *Transactions of ASME,* Vol. 74, No. 4, May 1952, pp. 473-497.

[4] Wood, H. J., "Current Technology of Radial Inflow Turbines for Compressible Fluids," *Journal of Engineering for Power, Transactions of ASME,* Vol. 85, Jan. 1963, pp. 72-83.

[5] Balje, O.E., "A Study on Design Criteria and Matching of Turbomachines: Part A-Similarity Relations and Design Criteria of Turbines," *Journal of Engineering for Power, Transactions of ASME,* Series A, Vol. 84, Jan. 1962, pp. 83-102.

[6] Vavra, M. H., "The Applicability of Similarity Parameters to the Compressible Flow in Radial Turbomachines," Paper No. 11, Institution of Mechanical Engineers Conference, Session 6, July 1967.

[7] Wallace, F.J., Baines, N.C., and Whitfield, A., "A Unified Approach to the One-Dimensional Analysis and Design of Radial and Mixed-Flow Turbines," ASME Paper 76-GR-100, March 1976.

[8] Benson, R.S., "A Review of Methods for Assessing Loss Coefficients in Radial Gas Turbines," *International Journal of Mechanical Science,* Vol. 12, Oct. 1970, pp. 905-932.

[9] Glassman, A.J., "Computer Program for Design Analysis of Radial Inflow Turbines," NASA TN D-8164, Feb. 1976.

[10] Rogers, C., "Advanced Radial Inflow Turbine Rotor Program – Design and Dynamic Testing," NASA CR-135080, Sept. 1976.

[11] Benedict, R.P., Carlucci, N.A., and Swetz, S.D., "Flow Losses in Abrupt Enlargements and Contractions," *Journal of Engineering for Power, Transactions of ASME,* Vol. 88, Jan. 1966, pp. 73-81.

[12] Stewart, W.L. "Analysis of Two-Dimensional Compressible Flow Loss Characteristics Downstream of Turbomachine Blade Rows in Terms of Basic Boundary Layer Characteristics," NACA TN-3515, July 1955, p. 155.

[13] Smith, L.H. Jr., "The Radial-Equilibrium Equation of Turbomachinery," *Journal of Engineering for Power, Transactions of ASME,* Vol. 88, Jan. 1966, pp. 1-12.

[14] Katsanis, T., "Use of Arbitrary Quasi-Orthogonals for Calculating Flow Distribution in the Meridional Plane of a Turbomachine," NASA TN D-2546, Dec. 1964.

[15] Stanitz, J.D. and Prian, V.D., "A Rapid Approximation Method for Determining Velocity Distribution on Impeller of Centrifugal Compressors," NACA TN 2421, July 1951.

[16] Sams, E.W., "Experimental Investigation of Average Heat Transfer and Friction Coefficients for Air Flowing in Circular Tubes Having Square Thread Type Roughness," NACA RME52D17, Lewis Flight Propulsion Lab., June 1952.

[17] Kolar, V., "Heat Transfer in Turbulent Flow of Fluids Through Smooth and Rough Pipes," *International Journal of Heat and Mass Transfer,* Vol. 8, No. 4, April 1965, pp. 639-653.

[18] Furber, B.N. and Cox, D.N., "Heat Transfer and Pressure Drop Measurements in Channels with Whitworth Thread Form Roughness," *Journal of Mechanical Engineering Science,* Vol. 9, No. 5, Dec. 1967, pp. 339-350.

[19] Norris, R.H., "Some Simple Approximate Heat-Transfer Correlation for Turbulent Flow in Ducts with Rough Surfaces," ASME Winter Meeting, Dec. 1970, printed in ASME Publication G76, "Augmentation of Convective Heat and Mass Transfer," 1970.

[20] Vershure, R.W. Jr., Fisk, H.R., and Vonada, J.A., "Demonstration of a Cooled Laminated Integral Axial Turbine," AIAA Paper 77-949; also *Journal of Aircraft,* Vol. 15, No. 11, 1978, pp. 735-742.

[21] Vershure, R.W. Jr., "Engine Demonstration Testing of a Cooled Laminated Axial Turbine," AIAA Paper 79-1229, June 1979.